

Enhanced Performance of $\text{LiNi}_{1/3}\text{Co}_{1/3}\text{Mn}_{1/3}\text{O}_2$ Cathodes at Elevated Temperatures Using an Imidazolium-Based Electrolyte with Lithium Difluoro(oxalate)Borate

Zhenfeng Wang, Jianhong Liu, Cuihua Li*, Peixin Zhang*, Haitao Zhuo

College of Chemistry and Environmental Engineering, Shenzhen University, No.3688, Nanhai District, Shenzhen 518060, China

*E-mail: licuihuasz@163.com, pxzhang2000@163.com

Received: 8 April 2016 / Accepted: 16 May 2016 / Published: 4 June 2016

Novel electrolytes containing 1,2-dimethyl-3-ethylimidazolium bis(trifluoromethylsulfonyl)imide, an ionic liquid (DMEITFSI); carbonate solvents; and lithium difluoro(oxalate)borate (LiDFOB) were prepared, and the electrochemical performance in $\text{Li}/\text{LiNi}_{1/3}\text{Co}_{1/3}\text{Mn}_{1/3}\text{O}_2$ half cells was investigated. The ionic liquid electrolytes exhibited excellent physical and electrochemical properties, including high thermal stability, incombustibility and a wide electrochemical window. The addition of LiDFOB significantly improved the compatibility of the ionic liquid with $\text{Li}/\text{LiNi}_{1/3}\text{Co}_{1/3}\text{Mn}_{1/3}\text{O}_2$, which presented a discharge capacity of 138.5 mAh g^{-1} after 100 cycles at 1.0 C. Among the tested electrolytes, $\text{Li}/\text{LiNi}_{1/3}\text{Co}_{1/3}\text{Mn}_{1/3}\text{O}_2$ cells showed the best performance at high temperatures, delivering superior discharge capacities of 157.7 mAh g^{-1} after 50 cycles at a rate of 1.0 C and a temperature of 80 °C. The decomposition of LiDFOB resulted in the formation of a stable and protective film on the surface of the $\text{LiNi}_{1/3}\text{Co}_{1/3}\text{Mn}_{1/3}\text{O}_2$ cathode. Therefore, nonflammable DMEITFSI-based electrolytes are an excellent alternative for lithium-ion batteries at room and elevated temperatures.

Keywords: Hybrid electrolyte, Ionic liquid, Safe electrolyte, High temperature, Lithium difluoro(oxalate)borate.

1. INTRODUCTION

Lithium-ion batteries (LIBs) have been widely used in various electronic devices; however, their energy and power density do not meet the demand of future electric vehicles and hybrid electric vehicles [1-3]. Recently, $\text{LiNi}_{1/3}\text{Co}_{1/3}\text{Mn}_{1/3}\text{O}_2$ has been shown to be an attractive cathode material for high-energy lithium batteries [4-6] due to its high specific capacity (180-200 mAh g^{-1}). Nevertheless, safety problems related to conventional electrolytes, including high flammability, low thermal stability and high vapor pressure, restrict the further development of $\text{LiNi}_{1/3}\text{Co}_{1/3}\text{Mn}_{1/3}\text{O}_2$ cathodes [7-9]. Thus,

a safe electrolyte with a wide electrochemical window and good electrode compatibility must be designed for LIBs.

Ionic liquids (ILs) have been investigated as safe electrolytes due to their wide liquid state range and electrochemical stability window, negligible volatility, non-flammability, etc. [10-13]. The most widely studied ILs for various applications are 1,3-dialkylimidazolium ILs, especially 1-ethyl-3-methylimidazolium ILs, due to its ease of preparation and low viscosity [14-17]. However, the presence of an active hydrogen at the C-2 position of the 1,3-dialkylimidazolium ring leads to electrochemical instability, which limits its usage in lithium batteries [18-20]. 1,2,3-Trialkylimidazolium ILs are produced after substituting the hydrogen at the C-2 position of the 1,3-dialkylimidazolium ring with an alkyl group. The resulting electrochemical stabilities are improved; thus, these ILs are attractive electrolytes for lithium batteries, even though their viscosities increase slightly with an increase in cation size [21].

Despite the outstanding stability of these ionic liquids, they also suffer from several disadvantages, such as high viscosity and poor compatibility with the cathode or anode due to the co-intercalation and decomposition of imidazolium cations on the surface of the electrode. The use of carbonate solvents and electrolyte additives are the most effective methods for solving the aforementioned disadvantages of ILs. For example, organic carbonates have been added to decrease the viscosity of neat ionic liquids and increase the electrode stability [22-24].

Lithium difluoro(oxalate)borate (LiDFOB) is an effective functional additive for improving cell performance [25-27]. Hu et al. [28] reported that the addition of LiDFOB improved the cyclic stability of LiCoPO_4 by forming a stable surface film, which passivated the cathode surface and inhibited electrolyte decomposition [29-31]. Independently, similar results were obtained by Chen et al. [32], confirming the ability of LiDFOB in carbonate-based electrolytes to support the cycling stability of $\text{LiNi}_{1/3}\text{Co}_{1/3}\text{Mn}_{1/3}\text{O}_2$ electrodes.

The effects of 1,2,3-trialkylimidazolium ionic liquid-based electrolytes on the electrode performance have only been marginally described in the literature. To date, studies on the addition of LiDFOB into 1,2-dimethyl-3-ethylimidazolium bis(trifluoromethylsulfonyl)imide (DMEITFSI)-based electrolytes and the effects on the electrochemical performance of $\text{LiNi}_{1/3}\text{Co}_{1/3}\text{Mn}_{1/3}\text{O}_2$ cathodes have seldom been reported. Therefore, the aim of the present study was to identify optimal DMEITFSI-based electrolytes for high capacity LiDFOB cathodes at room and elevated temperature and to better understand the effects of IL and LiDFOB on $\text{LiNi}_{1/3}\text{Co}_{1/3}\text{Mn}_{1/3}\text{O}_2$ cathodes. The physical and electrochemical properties of ionic liquid electrolytes containing DMEITFSI, lithium bis(trifluoromethanesulfonyl)imide (LiTFSI) and LiDFOB were evaluated. Particularly, the cyclic performance of DMEITFSI-based electrolytes in $\text{Li}/\text{LiNi}_{1/3}\text{Co}_{1/3}\text{Mn}_{1/3}\text{O}_2$ half cells at temperatures of 70 and 80 °C was explored.

2. EXPERIMENTAL

2.1 Synthesis of DMEITFSI

DMEITFSI, which is shown in Fig. 1, was synthesized according to the following route: bromoethane (7.4 mL, 0.1 mol, Alfa Aesar, >98%) and 1,2-dimethylimidazole (9.0 mL, 0.1 mol, Alfa

Aesar, >98%) were dissolved in ethyl acetate (25 mL) and stirred overnight at 25 °C. After purification by washing with ethyl acetate, the intermediate 1,2-dimethyl-3-ethylimidazolium bromide (DMEIBr) was obtained as a white solid in 91% yield (18.6 g). Subsequently, 18.6 g of DMEIBr, which was produced in the first step, was dissolved in 10 mL of deionized water, and the resulting mixture was added into a solution of 28.7 g of LiTFSI (Acros, >98%) in 10 mL of deionized water. The mixture was stirred at 25 °C for 24 h.

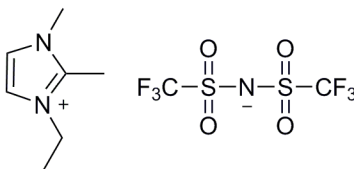


Figure 1. The chemical structure of DMEITFSI

The product of this reaction, DMEITFSI, was removed and washed several times with deionized water until bromide was not detected by titration with 0.1 mol L⁻¹ AgNO₃. The remaining water was removed under vacuum at 110°C for 48 hours. The final product was a clear colorless liquid (yield: 35.3 g, 87.0%). The water content was less than 50 ppm and was measured via Karl Fischer analysis. The purity of the IL was determined using ¹H nuclear magnetic resonance (¹H NMR) on a 400 MHz spectrometer (VNMRs 400, Varian). The chemical shifts are reported in ppm downfield from tetramethylsilane. DMEITFSI δ_H (400 MHz, DMSO-d₆): 7.65 (d, *J*=1.8 Hz, 1H), 7.64–7.57 (m, 1H), 4.13 (dd, *J*=14.2, 7.0 Hz, 2H), 3.75 (d, *J*=5.7 Hz, 3H), 2.58 (d, *J*=5.7 Hz, 3H), 1.34 (t, *J*=7.2 Hz, 3H).

2.2 Preparation of DMEITFSI-based electrolytes and half cells

LiDFOB (Beijing Isomersyn Technology Co., Ltd., China), dimethyl carbonate (DMC, Shenzhen Tianjiao Sources Technology Co., Ltd., China) and vinylene carbonate (VC, Acros, >98%) were used as received. DMEITFSI-based electrolytes with a composition and systematic nomenclature of 0.3 M LiTFSI/δ vol% DMEITFSI+(95-δ) vol% DMC+5 vol% VC+0.25 wt% LiDFOB were prepared with δ values ranging from 70 to 90. These DMEITFSI-based electrolytes were indicated by 70, 80 and 90 vol% IL. The other DMEITFSI-based electrolyte consisted of 0.3 M LiTFSI/DMEITFSI+5 vol% VC+0.25 wt% LiDFOB was also prepared and named as 100 vol% IL. A conventional electrolyte, which consisted of 1 M LiPF₆-EC/DMC/EMC (1/1/1, v/v/v), was used for comparison. The HF and water content of the electrolytes were less than 50 ppm, which determined by Karl-Fisher titration. The electrode with an active loading of about 2.3 mg cm⁻² was prepared using a mixture of 80 wt% LiNi_{1/3}Co_{1/3}Mn_{1/3}O₂, 10 wt% carbon black, and 10 wt% poly(vinylidenedifluoride)binder in N-methyl-2-pyrrolidone. The resulting slurry was cast on a circular Al foil with a diameter of 14 mm. All of the electrodes were dried under vacuum at 110 °C for at least 12 h prior to use. The 2032-type coin cells were assembled with the aforementioned electrode, lithium foil as counter electrode and Celgard 2400 membrane as separator in a glove box under an Ar

atmosphere ($O_2 < 0.1$ ppm, $H_2O < 0.1$ ppm; UNILab, Mbraun). Same amount of electrolyte of 55 μ L was used for each coin cell.

2.3 Physical-chemical characterization and evaluation of the cells

The flammability of the electrolytes was evaluated according to the method described in our previous study [33]. Briefly, 200 μ L of electrolyte was added into an stainless steel container and was carefully ignited. The electrolyte was judged to be non-flammable if the electrolyte did not ignite during testing. The thermogravimetric analysis (TGA) of DMEITFSI-based electrolytes was carried out using a thermal analysis system (Q50, TA instruments) under a nitrogen atmosphere at room temperature to 640 $^{\circ}$ C and a heating rate of 5 $^{\circ}$ C min^{-1} . The viscosity of DMEITFSI-based electrolytes was measured at 25 ± 1 $^{\circ}$ C using a rotational viscometer (AR1000, TA instruments) with a cone-plate configuration in control shear rate mode. The contact angle between DMEITFSI-based electrolytes and the separator was measured using a contact angle meter (JC2000C1, POWEREACH).

The ionic conductivity of DMEITFSI-based electrolytes was measured by AC impedance spectroscopy on an electrochemical workstation (1470E Cell Test System, Solartron) using a two Pt-electrode cell. Electrochemical measurements, including electrochemical impedance spectroscopy (EIS), linear sweep voltammetry (LSV) and cyclic voltammetry (CV) were measured in coin-type cells on the aforementioned electrochemical workstation (1470E Cell Test System, Solartron). The EIS of Li/LiNi $_{1/3}$ Co $_{1/3}$ Mn $_{1/3}$ O $_2$ cells at various cycles was tested in a frequency range of 10^5 Hz to 10^{-2} Hz with an amplitude of 10 mV. The CV of Li/LiNi $_{1/3}$ Co $_{1/3}$ Mn $_{1/3}$ O $_2$ cells was measured at 2.75-4.5 V and a scan rate of 0.1 mV s^{-1} . The electrochemical stability of the electrolytes was tested via LSV in Li/Pt cells at 0 to 6 V and a scan rate of 0.1 mV s^{-1} . The cycling performance of Li/LiNi $_{1/3}$ Co $_{1/3}$ Mn $_{1/3}$ O $_2$ cells containing the studied electrolytes was determined using a Land CT2001A battery testing system at different rates and voltages of 2.75-4.5 V. A scanning electron microscope (SEM, S3400N, Hitachi) coupled with an energy dispersive spectrometer (EDS) was used to investigate the surface morphology and composition of pristine and cycled electrodes.

3. RESULTS AND DISCUSSION

3.1 Physical and electrochemical properties

The flammability and thermal stability of electrolytes are the primary factors affecting battery safety. We observed that the as-prepared electrolytes were non-flammable and could meet the safety demands when the IL content was set to 70 vol% (This result is not shown here).

Thus, only the physical and electrochemical performance of electrolytes with DMEITFSI contents greater than over 70 vol% were investigated herein. The TGA analysis of electrolytes with different DMEITFSI contents is shown in Fig. 2A. Significant weight loss was not observed for the IL electrolyte without carbonate solvent at temperatures up to 320 $^{\circ}$ C, which indicated the high thermal stability of DMEITFSI. In contrast, a weight loss of 43.8 wt% was obtained when the conventional

carbonate-based electrolyte was heated from 20 to 100 °C. For electrolytes with 70, 80, and 90 vol% IL, the weight losses were 14.0, 7.7 and 4.7 wt%, respectively. The volatility of the carbonate solvent decreased due to the addition of the ionic liquid, which was attributed to the strong intermolecular forces between the IL and organic solvent [34].

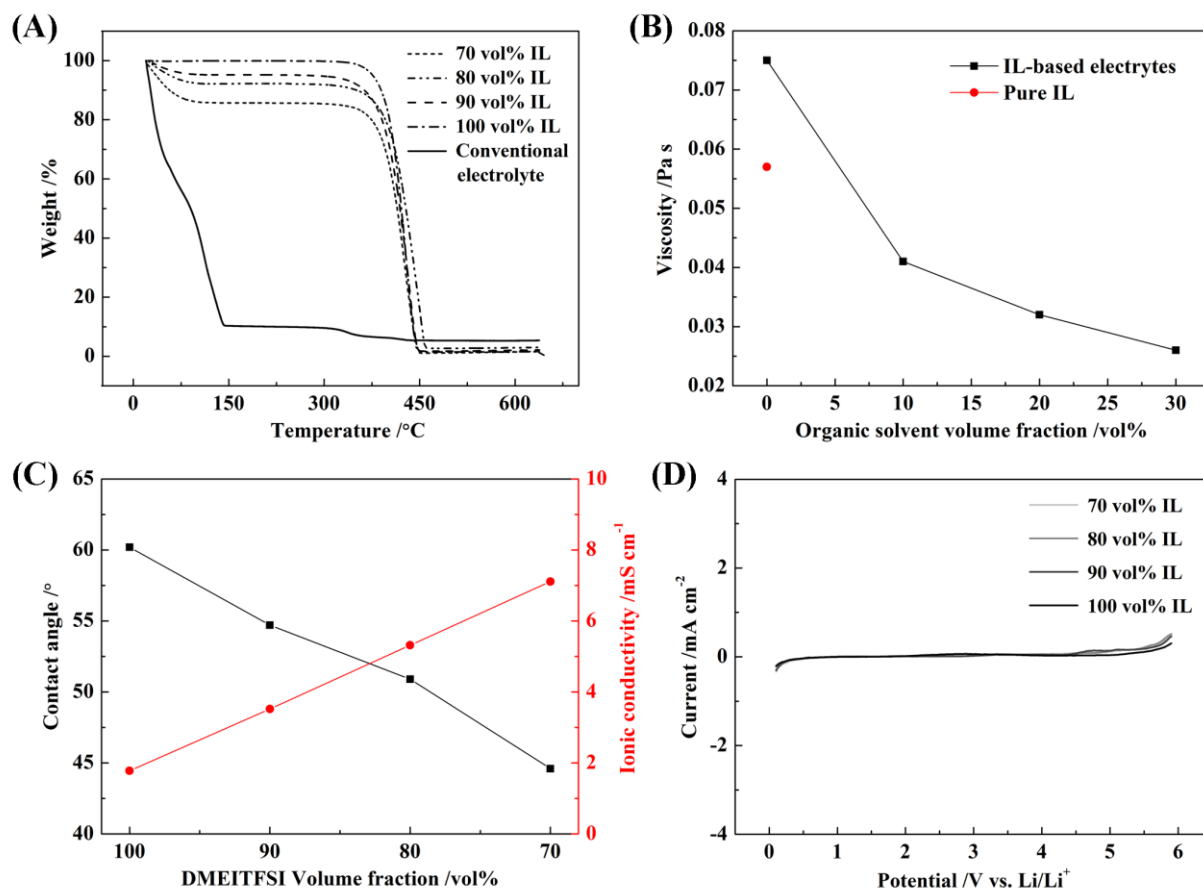


Figure 2. Physical and electrochemical properties of IL-based electrolytes: (A) thermogravimetric analysis, (B) viscosity, (C) contact angle and conductivity and (D) linear sweep voltammograms

The viscosity of the mixed electrolytes and pure IL is presented in Fig. 2B. DMEITFSI displayed a relatively high viscosity, and the addition of lithium salts to the IL increased the viscosity. One method of decreasing the viscosity of a liquid is to add an organic solvent such as DMC. The addition of 10 vol% DMC to the electrolyte significantly decreased the viscosity by 45%. As the amount of DMC in the electrolyte increased, the viscosity of the electrolyte decreased gradually because interaction forces among molecules in the electrolyte also decreased upon DMC addition [35].

Fig. 2C shows the relationship between the contact angle and conductivity of the electrolyte at various IL concentrations. The contact angle of the electrolyte with 70, 80, 90 and 100 vol% of DMEITFSI was 44.6°, 50.9°, 54.7° and 60.2°, respectively. As the content of DMEITFSI in the electrolyte decreased, a gradual decrease in the contact angle was observed. Thus, the contact angle of

the mixture was positively correlated with the viscosity. The electrolyte containing 70, 80, 90 and 100 vol% of DMEITFSI displayed conductivities of 7.11, 5.32, 3.52 and 1.78 mS cm⁻¹, respectively. Notably, the conductivity of the mixtures was inversely correlated to the viscosity.

The electrochemical stability of neat DMEITFSI and DMEITFSI-based electrolytes was measured by LSV. As shown in Fig. 2D, oxidation and reduction peaks were not observed in the range of 0 to 5.5 V for all of the tested cells, indicating that the electrochemical stability of DMEITFSI-based electrolytes was high, even when the concentration of organic solvents was set to contents as high as 30 vol%. This result confirmed the feasibility of DMEITFSI-based electrolytes for lithium-ion batteries.

3.2 Cyclic performance of Li/LiNi_{1/3}Co_{1/3}Mn_{1/3}O₂ cells at room temperature

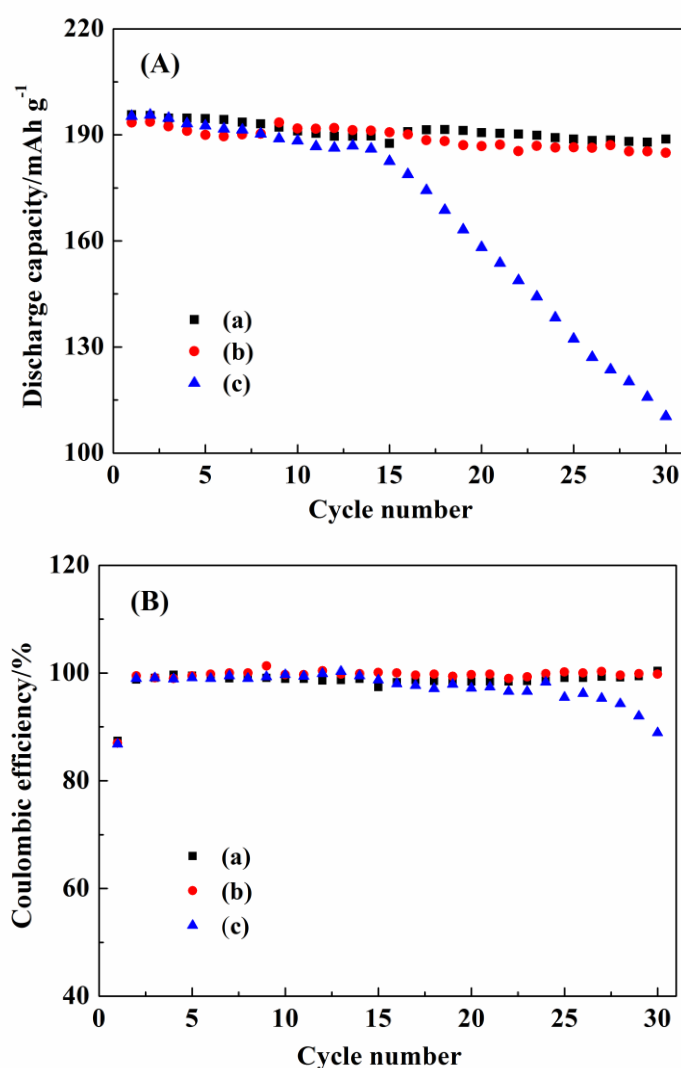


Figure 3. Cyclic performance (A) and coulombic efficiency (B) of Li/LiNi_{1/3}Mn_{1/3}Co_{1/3}O₂ at a voltage range of 2.75–4.5 V, a rate of 0.10 C and a temperature of 25 °C: (a) conventional electrolyte, (b) 0.3 M LiTFSI/70 vol% IL+25 vol% DMC+5 vol% VC+0.25 wt% LiDFOB and (c) 0.3 M LiTFSI/70 vol% IL+25 vol% DMC+5 vol% VC

Fig. 3 shows the cyclic performance of Li/LiNi_{1/3}Co_{1/3}Mn_{1/3}O₂ cells in different electrolytes at a temperature of 25 °C, a rate of 0.1 C and a voltage range of 2.75-4.5 V. Electrolyte (b), which contained LiDFOB and DMC, exhibited excellent performance, similar to the conventional carbonate electrolyte (a). Compared to electrolyte (b), the discharge capacity decreased dramatically in the absence of LiDFOB, and a low capacity of 110.4 mAh g⁻¹ was obtained after 30 cycles due to the decomposition of DMEI⁺ on the surface of the electrode [22]. The addition of LiDFOB to the electrolyte (c) prevented the above-mentioned process and resulted in the formation of a stable SEI film on the surface of the LiNi_{1/3}Co_{1/3}Mn_{1/3}O₂ electrode. With respect to safety, the optimal electrolyte composition included DMEITFSI, DMC and LiDFOB (0.3 M LiTFSI/δ vol% DMEITFSI + (95-δ) vol% DMC + 5 vol% VC+0.25 wt% LiDFOB). Thus, this type of electrolyte was used in the following tests.

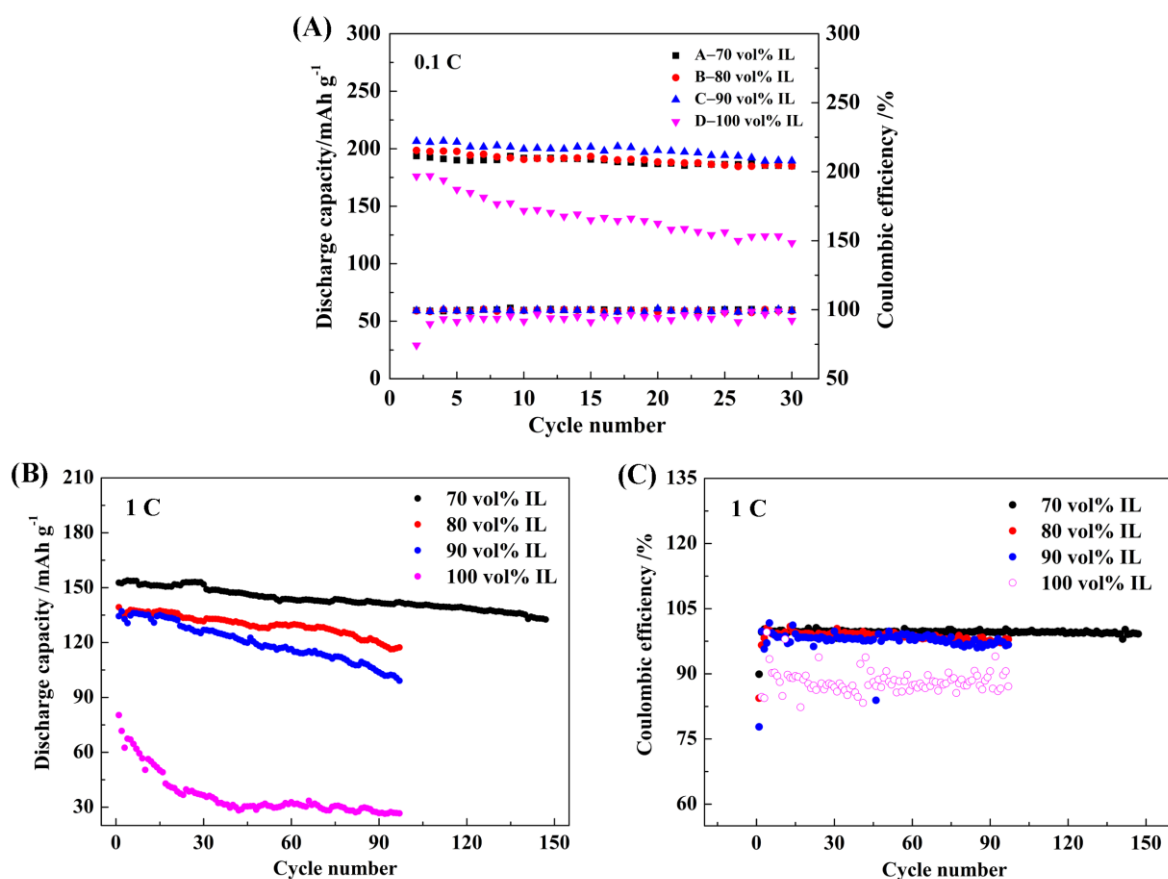


Figure 4. Cyclic performance of LiNi_{1/3}Mn_{1/3}Co_{1/3}O₂ in IL-based electrolytes containing LiDFOB at 25 °C and 0.1 C and 1.0 C

As shown in Fig. 4A, the initial discharge capacity of Li/LiNi_{1/3}Co_{1/3}Mn_{1/3}O₂ cells reached 193.5 mAh g⁻¹. The capacity retention and coulombic efficiency for A, B and C was greater than 93.0% and 99.9%, respectively, after 30 cycles at 0.1 C, which indicated that the addition of DMEITFSI and LiDFOB to the electrolyte increased the discharge capacities and coulombic efficiencies of Li/LiNi_{1/3}Co_{1/3}Mn_{1/3}O₂. Cells containing 100 vol% IL electrolyte showed poor discharge capacities

and coulombic efficiencies due to the high viscosity of the electrolyte, which reduced the migration rate of Li^+ . The observed side effects of high viscosity are evident in Fig. 4B, which shows the performance characteristics obtained at a rate of 1.0 C, voltages ranging from 2.75-4.5 V and a temperature of 25 °C. Throughout the entire 150-cycle experiment, the electrolyte containing 70 vol% IL showed superior performance compared to the electrolyte with 80 and 90 vol% DMEITFSI. As the amount of DMEITFSI in the electrolyte increased, the discharge capacities of the cell decreased gradually at room temperature.

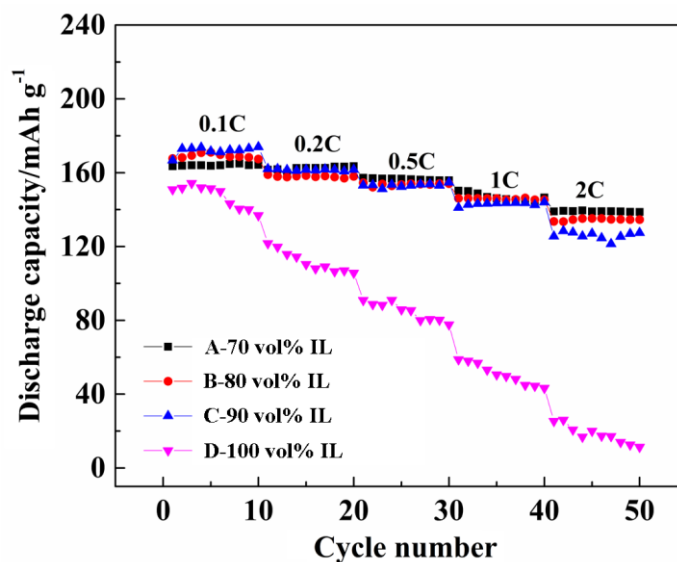


Figure 5. Rate performance of $\text{Li}/\text{LiNi}_{1/3}\text{Mn}_{1/3}\text{Co}_{1/3}\text{O}_2$ cells using IL-based electrolytes containing LiDFOB at 25 °C

The rate capability is an important factor affecting the cyclic performance. The rate performance of $\text{Li}/\text{LiNi}_{1/3}\text{Co}_{1/3}\text{Mn}_{1/3}\text{O}_2$ cells with DMEITFSI-based electrolytes is shown in Fig. 5. The rate capabilities of the cells decreased according in the following order: Cell A (70 vol% IL) > Cell B (80 vol% IL) > Cell C (90 vol% IL) > Cell D (100 vol% IL). The discharge capacity of the cell containing 100 vol% IL electrolyte (Cell D) rapidly decreased to 25.4 mAh g^{-1} at 2.0 C, which was only 16.8% of the discharge capacity at 0.1 C. Cell A (70 vol% IL), Cell B (80 vol% IL) and Cell C (90 vol% IL) exhibited comparable discharge capacities of 139.0, 133.6 and 125.5 mAh g^{-1} , respectively, up to a rate of 2.0 C. The rate performance of the cathode in 70-90 vol% DMEITFSI-based electrolyte was sufficient for many applications.

3.3 Cyclic performance of $\text{Li}/\text{LiNi}_{1/3}\text{Co}_{1/3}\text{Mn}_{1/3}\text{O}_2$ cells at elevated temperature

Fig. 6 shows the cyclic performance of $\text{LiNi}_{1/3}\text{Co}_{1/3}\text{Mn}_{1/3}\text{O}_2$ in electrolytes with different concentrations of DMEITFSI at high temperatures and a voltage range of 2.75 to 4.5 V. The discharge capacities of the cell improved significantly as the temperature increased. Compared to cells evaluated at 25 °C, the discharge capacity increased by 14.8% (70 vol% IL), 26.3% (80 vol% IL), 29.9% (90

vol% IL) at 70 °C and 9.9% (70 vol% IL), 26.6% (80 vol% IL), 28.8% (90 vol% IL) at 80 °C, respectively. In addition, improved capacity retention was achieved in cells cycled in larger amounts of IL at higher temperatures.

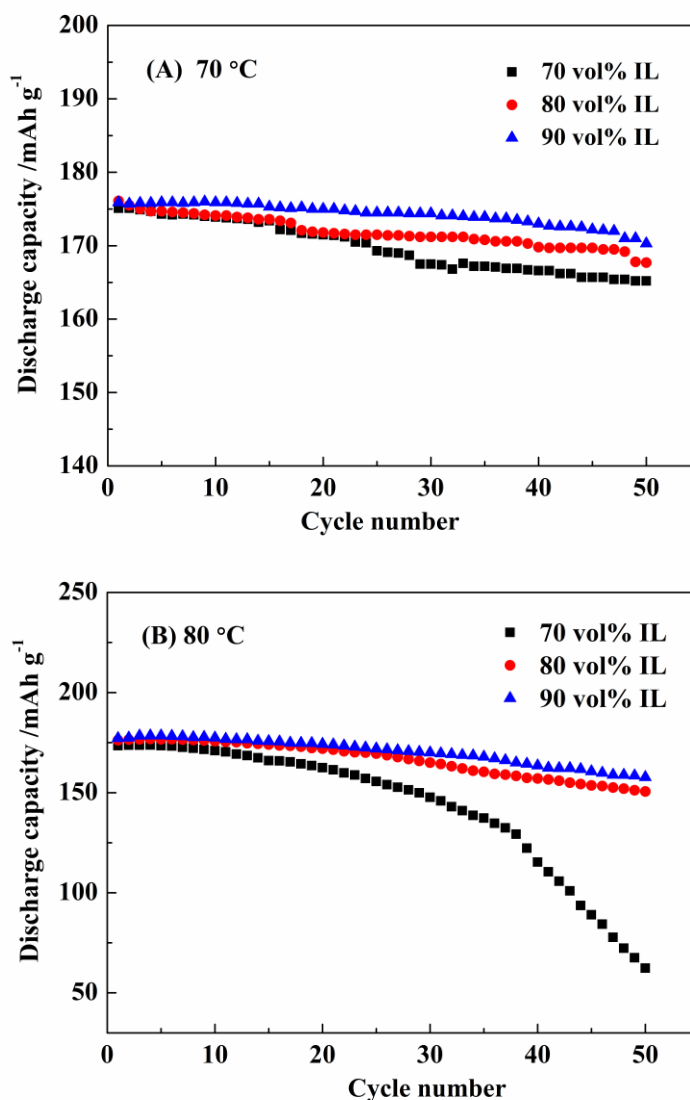


Figure 6. Cyclic performance of Li/LiNi_{1/3}Mn_{1/3}Co_{1/3}O₂ cells in IL-based electrolytes containing LiDFOB at 1.0 C and (A) 70 °C and (B) 80 °C

For example, the capacity loss of the cell containing 90 vol% IL after 50 cycles at 80 °C was only 19.5 mAh g⁻¹ at 1.0 C (from 177.2 mAh g⁻¹ to 157.7 mAh g⁻¹), while the capacity loss of the cell containing 70 vol% IL was 111.2 mAh g⁻¹ (from 173.5 mAh g⁻¹ to 62.3 mAh g⁻¹), indicating that electrolytes with higher IL contents displayed greater discharge capacities and superior capacity retentions at high temperatures. This result was attributed to two factors. Namely, with larger amounts of IL, intermolecular forces in the electrolyte decreased faster when the temperature increased, which led to a faster migration rate of Li⁺ and improved discharge capacities and capacity retentions. Alternatively, the evaporation of DMC at 70 and 80 °C may have significantly reduced the discharge

capacity. DMEITFSI-based electrolytes with higher IL contents provided better compatibility with $\text{LiNi}_{1/3}\text{Co}_{1/3}\text{Mn}_{1/3}\text{O}_2$ at high temperature and may be a promising choice for lithium-ion batteries at high temperature.

3.4 Electrochemical behavior of $\text{LiNi}_{1/3}\text{Co}_{1/3}\text{Mn}_{1/3}\text{O}_2$ cathodes

The CV curves of $\text{LiNi}_{1/3}\text{Co}_{1/3}\text{Mn}_{1/3}\text{O}_2$ cells containing electrolyte with and without LiDFOB are provided in Fig. 7.

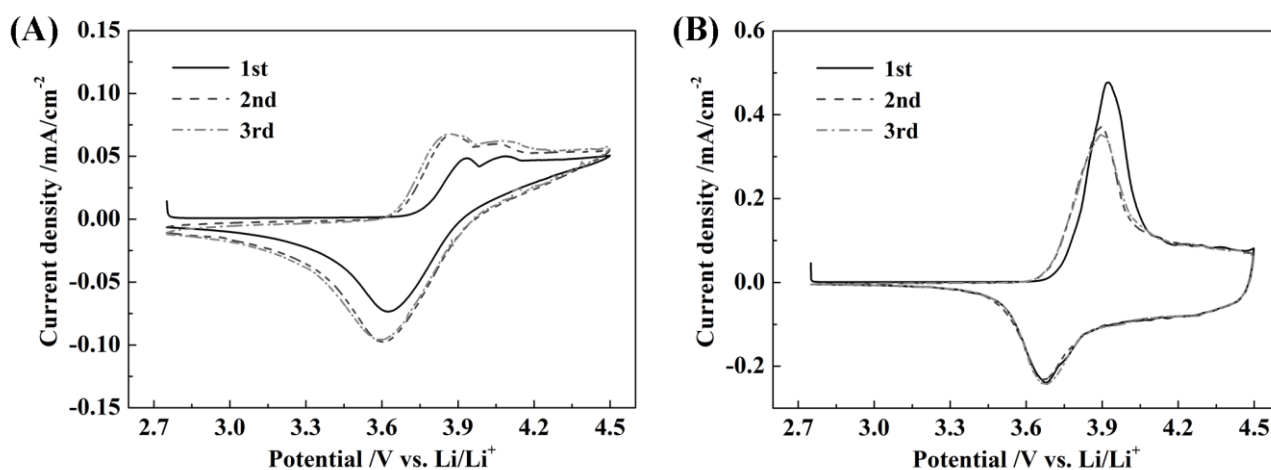


Figure 7. Cyclic voltammograms of $\text{Li}/\text{LiNi}_{1/3}\text{Mn}_{1/3}\text{Co}_{1/3}\text{O}_2$ cells containing (A) standard electrolyte and (B) electrolyte with LiDFOB at 0.1 mV s^{-1}

As shown in Fig. 7A, a broad anodic peak was observed at 3.9-4.5 V in the first circle, which was attributed to the oxidation reaction between the electrolyte and the electrode. After the second scan, the electrochemical behavior of the $\text{LiNi}_{1/3}\text{Co}_{1/3}\text{Mn}_{1/3}\text{O}_2$ electrode was poor. The electrochemical profiles of $\text{LiNi}_{1/3}\text{Co}_{1/3}\text{Mn}_{1/3}\text{O}_2$ electrodes containing LiDFOB (Fig. 7B) showed a sharp oxidation peak at 3.92 V in the first positive scan, corresponding to the oxidation of Ni^{2+} and Co^{3+} to Ni^{4+} and Co^{4+} , respectively. The reduction peak at 3.68 V was due to the reduction of Ni^{4+} and Co^{4+} [10]. After the first cycle, the current density of the oxidation process decreased slightly but remained stable in the next cycle, suggesting that lithium insertion and extraction from the $\text{LiNi}_{1/3}\text{Co}_{1/3}\text{Mn}_{1/3}\text{O}_2$ electrode was highly reversible. Therefore, the addition of LiDFOB suppressed undesirable interfacial reactions between the electrolyte and electrode.

The electrochemical impedance spectra of $\text{Li}/\text{LiNi}_{1/3}\text{Co}_{1/3}\text{Mn}_{1/3}\text{O}_2$ cells were collected after the 1st, 5th, 10th and 15th cycle at 1.0 C and 25 °C (Fig. 8A and B). The EIS spectra were fitted with the equivalent circuit inserted in Fig. 8A and the values of R_s , R_f and R_{ct} were listed in Table 1. As previously reported, R_s represents the resistance contribution from the electrolyte and cell case, R_f is the resistance of the film formed on the surface of the cathode, and R_{ct} is related to the resistance of the charge transfer process [37].

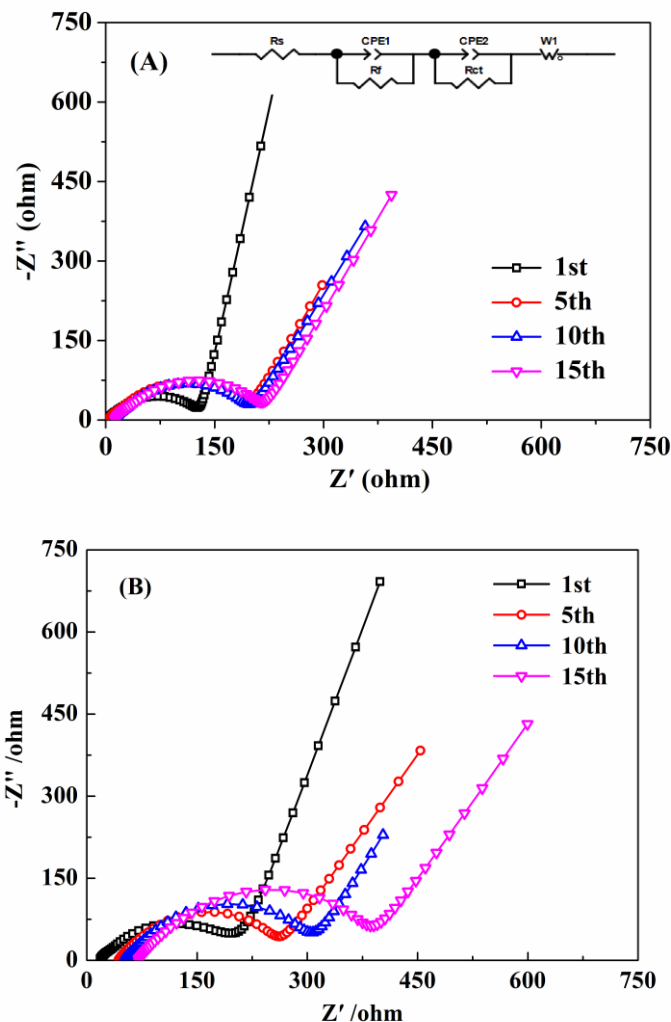


Figure 8. EIS plots of Li/LiNi_{1/3}Mn_{1/3}Co_{1/3}O₂ cells in IL-based electrolytes containing LiDFOB. (A) 70 vol% IL and (B) 90 vol% IL

Table 1. Impedance parameters calculated by equivalent circuits in IL-based electrolytes with LiDFOB

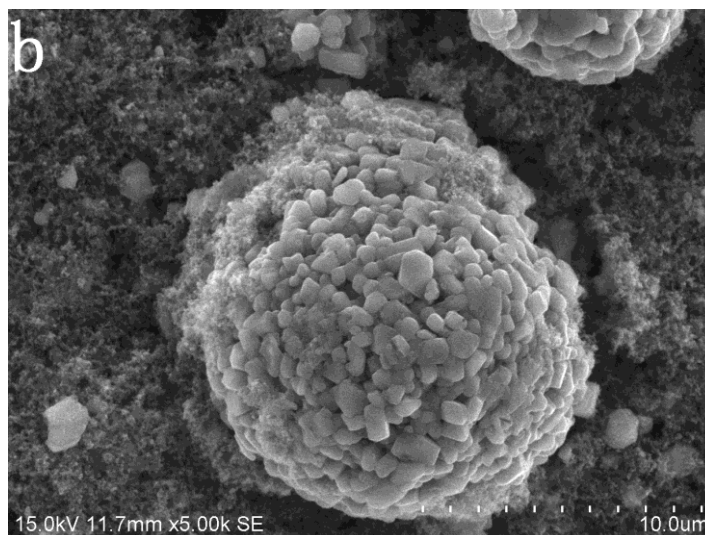
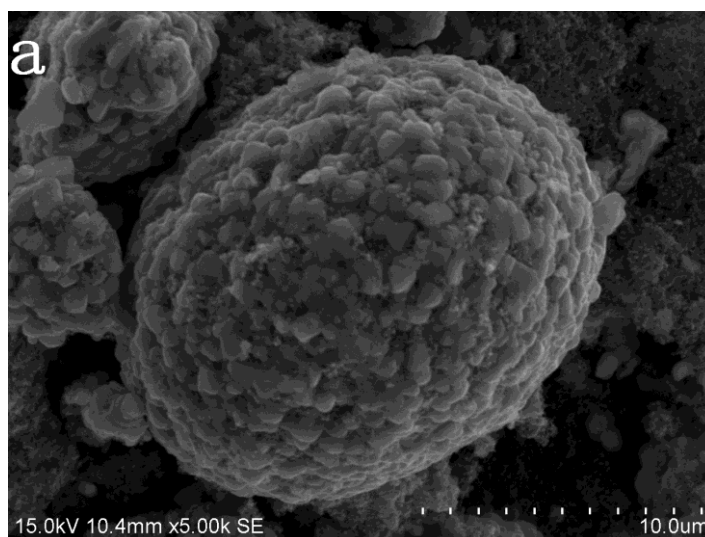
Sample	R _s /Ω	R _f /Ω	R _{ct} /Ω
70vol% IL(1st)	4.059	7.138	119
70vol% IL(5th)	4.596	14.76	173.7
70vol% IL (10th)	12.44	14.57	168.7
70vol% IL (15th)	12.87	23.88	176.1
90vol% IL (1st)	16.74	8.954	135.1
90 vol% IL (5th)	42.38	56.83	152.5
90 vol% IL (10th)	49.11	60.43	179.7
90 vol% IL (15th)	68.39	91.39	201.1

For cell cycled in the electrolyte containing 90 vol% IL, R_s, R_f and R_{ct} remarkably increased as cycling proceeded. This is probably due to the high viscosity of 90 vol% IL electrolyte, which blocks the Li⁺ transport. For cell cycled in the electrolyte containing 70 vol% IL, while R_f and R_{ct} increased

slightly with cycling, much smaller values of R_s than those cycled in the electrolyte containing 90 vol% IL, indicating that the 70 vol% electrolyte shows good compatibility with $\text{LiNi}_{1/3}\text{Co}_{1/3}\text{Mn}_{1/3}\text{O}_2$ cathode. Since appropriate amount of DMC decrease the viscosity of the electrolyte, Li^+ is able to be more easily transfer to the electrode surface and then enter the structure of the electrode. As a result, the cell with 70 vol% IL electrolyte exhibits better cyclic performance.

3.5 Surface analysis of $\text{LiNi}_{1/3}\text{Co}_{1/3}\text{Mn}_{1/3}\text{O}_2$ cathodes

SEM images of pristine and cycled $\text{LiNi}_{1/3}\text{Co}_{1/3}\text{Mn}_{1/3}\text{O}_2$ cathodes are presented in Fig. 9. The pristine electrode showed a uniformly distributed spherical or near spherical morphology (Fig. 9a). After 30 cycles, the surface of the electrode without LiDFOB maintained its initial morphology, but a limited number of close spherical particles became loose (Fig. 9b). In contrast, the spherical particles of the electrode cycled with LiDFOB were covered with a thick SEI layer and remained cohesive, as observed in Fig. 9c.



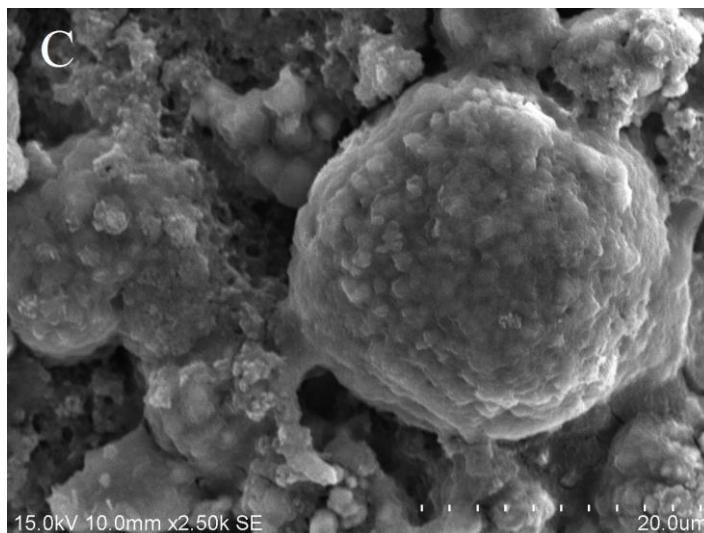


Figure 9. SEM images of pristine $\text{LiNi}_{1/3}\text{Mn}_{1/3}\text{Co}_{1/3}\text{O}_2$ cathodes (a) and cycled $\text{LiNi}_{1/3}\text{Mn}_{1/3}\text{Co}_{1/3}\text{O}_2$ cathodes after 30 cycles using (b) LiDFOB-free and (c) LiDFOB-based electrolytes

The addition of LiDFOB led to the formation of a stable interphase film and passivated the surface of the $\text{LiNi}_{1/3}\text{Co}_{1/3}\text{Mn}_{1/3}\text{O}_2$ cathode [28]. Therefore, DMEITFSI-based electrolytes containing LiDFOB were compatible with $\text{LiNi}_{1/3}\text{Co}_{1/3}\text{Mn}_{1/3}\text{O}_2$. This observation is in accordance with the galvanostatic measurements.

Energy dispersive spectroscopy is a useful tool for the compositional analysis of solid surfaces [41, 42]. The concentrations of elements observed on the electrode surface are shown in Table 2.

Compared to fresh electrodes and electrodes cycled without LiDFOB, electrodes cycled with LiDFOB possessed lower Co, Mn and Ni contents and higher B and O contents, which was indicative of the irreversible decomposition of LiDFOB on the surface of the electrode. Similar results were obtained in Li/LiCoPO₄ cells cycled with carbonate-based electrolyte containing LiDFOB [28]. The observed increase in the B content was consistent with the CV curves of $\text{LiNi}_{1/3}\text{Co}_{1/3}\text{Mn}_{1/3}\text{O}_2$ shown in Fig. 7B. These results suggested that LiDFOB decomposed during the process and assisted in the formation of a compact and stable interphase film on the surface of the $\text{LiNi}_{1/3}\text{Co}_{1/3}\text{Mn}_{1/3}\text{O}_2$ cathode, which passivated the cathode surface and reduced the decomposition of DMEI⁺ on the surface of the $\text{LiNi}_{1/3}\text{Co}_{1/3}\text{Mn}_{1/3}\text{O}_2$ cathode.

Table 2. Surface concentration of the elements in the fresh and cycled $\text{LiNi}_{1/3}\text{Mn}_{1/3}\text{Co}_{1/3}\text{O}_2$ cathodes in the electrolytes with or without LiDFOB

Sample	C	O	F	B	Mn	Ni	Co
Fresh cathode	15.55	32.67	7.15	0	12.47	23.05	9.10
Cycled cathode without LiDFOB	13.76	34.57	6.89	0	12.29	23.28	9.22
Cycled cathode with LiDFOB	14.35	43.87	5.15	1.94	9.22	18.20	7.26

4. CONCLUSIONS

Novel electrolytes based on DMEITFSI, DMC and LiDFOB were prepared for Li/LiNi_{1/3}Co_{1/3}Mn_{1/3}O₂ half cells and exhibited enhanced safety and good compatibility with LiNi_{1/3}Co_{1/3}Mn_{1/3}O₂ cathodes at room and elevated temperatures. The optimal composition of DMEITFSI-based electrolytes was explored based on their electrochemical performance. The electrolyte containing DMEITFSI and LiDFOB showed high conductivity (7.11 mS cm⁻¹ at 25 °C), low viscosity (0.026 Pa s), high thermal stability (up to 320 °C) and a large overall stability window of more than 5.5 V. The cyclic performance of the electrolyte in Li/LiNi_{1/3}Co_{1/3}Mn_{1/3}O₂ half cells was also encouraging, showing a discharge capacity of ca. 132.6 mAh g⁻¹ after 150 cycles at 1.0 C and 25 °C, which was comparable to the performance of conventional carbonate-based electrolytes. Cells containing Li/LiNi_{1/3}Co_{1/3}Mn_{1/3}O₂, 90 vol% IL and LiDFOB delivered a discharge capacity of 177.2 mAh g⁻¹ and a capacity retention of 89.0% at 1.0 C after 50 cycles at 80 °C. The presence of LiDFOB in the electrolyte resulted in the formation of a compact and stable SEI film, which reduced the decomposition of DMEI⁺ on the surface of the LiNi_{1/3}Co_{1/3}Mn_{1/3}O₂ cathode, leading to enhanced electrochemical performance and stability at high temperature.

ACKNOWLEDGEMENT

This work was financially supported by National Natural Science Foundation (51574166) and Scientific and Technological Research and Development Foundation of Shenzhen City (JCYJ20140418193546111).

References

1. M. Armand and J-M. Tarascon, *Nature*, 451 (2008) 652-657.
2. A.S. Aricò, P. Bruce, B. Scrosati, J-M. Tarascon and W. Van Schalkwijk, *Nat. Mater.*, 4 (2005) 366-377.
3. L. Su, Y. Jing and Z. Zhou, *Nanoscale*, 3 (2011) 3967-3983.
4. Q. Wu, W. Lu, M. Miranda, T.K. Honaker-Schroeder, K.Y. Lakhsassi and D. Dees, *Electrochem. Commun.*, 24 (2012) 78-81.
5. C.S. Johnson, J.S. Kim, C. Lefief, N. Li, J.T. Vaughey and M.M. Thackeray, *Electrochem. Commun.*, 6 (2004) 1085-1091.
6. J-H. Lim, H. Bang, K-S. Lee, K. Amine and Y-K. Sun, *J. Power Sources*, 189 (2009) 571-575.
7. M. Wang, Z. Shan, J. Tian, K. Yang, X. Liu, H. Liu and K. Zhu, *Electrochim. Acta*, 95 (2013) 301-307.
8. P.G. Balakrishnan, R. Ramesh and T. Prem Kumar, *J. Power Sources*, 155 (2006) 401-414.
9. J.B. Goodenough and Y. Kim, *Chem. Mater.*, 22 (2009) 587-603.
10. H. Li, J. Pang, Y. Yin, W. Zhuang, H. Wang, C. Zhai and S. Lu, *RSC Adv.*, 3 (2013) 13907-13914.
11. H. Nakagawa, Y. Fujino, S. Kozono, Y. Katayama, T. Nukuda, H. Sakaebe, H. Matsumoto and K. Tatsumi, *J. Power Sources*, 174 (2007) 1021-1026.
12. Y. Jin, S. Fang, M. Chai, L. Yang, K. Tachibana and S. Hirano, *J. Power Sources*, 226 (2013) 210-218.
13. X-G. Sun, C. Liao, N. Shao, J.R. Bell, B. Guo, H. Luo, D. Jiang and S. Dai, *J. Power Sources*, 237 (2013) 5-12.
14. S.A. Forsyth, J.M. Pringle and D.R. MacFarlane, *Aust. J. Chem.*, 57 (2004) 113-119.

15. J. Ranke, S. Stolte, R. Störmann, J. Arning and B. Jastorff, *Chem. Rev.*, 107 (2007) 2183-2206.
16. J. Dupont and J.D. Scholten, *Chem. Soc. Rev.*, 39 (2010) 1780-1804.
17. J-K. Kim, A. Matic, J-H. Ahn and P. Jacobsson, *J. Power Sources*, 195 (2010) 7639-7643.
18. H. Saruwatari, T. Kuboki, T. Kishi, S. Mikoshiba and N. Takami, *J. Power Sources*, 195 (2010) 1495-1499.
19. I.A. Profatilova, N-S. Choi, S.W. Roh and S.S. Kim, *J. Power Sources*, 192 (2009) 636-643.
20. M. Egashira, H. Todo, N. Yoshimoto, M. Morita and J-I. Yamaki, *J. Power Sources*, 174 (2007) 560-564.
21. Y. Jin, S. Fang, M. Chai, L. Yang, K. Tachibana and S. Hirano, *J. Power Sources*, 226 (2013) 210-218.
22. J. Reiter, M. Nadherná and R. Dominko, *J. Power Sources*, 205 (2012) 402-407.
23. H. Zheng, K. Jiang, T. Abe and Z. Ogumi, *Carbon*, 44 (2006) 203-210.
24. X-G. Sun and S. Dai, *Electrochim. Acta*, 55 (2010) 4618-4626.
25. J. Liu, Z. Chen, S. Busking and K. Amine, *Electrochem. Commun.*, 9 (2007) 475-479.
26. J. Liu, Z. Chen, S. Busking, I. Belharouak and K. Amine, *J. Power Sources*, 174 (2007) 852-855.
27. J. Li, K. Xie, Y. Lai, Z.A. Zhang, F. Li, X. Hao, X. Chen and Y. Liu, *J. Power Sources*, 195 (2010) 5344-5350.
28. M. Hu, J. Wei, L. Xing and Z. Zhou, *J. Appl. Electrochem.*, 42 (2012) 291-296.
29. Y. Zhu, Y. Li, M. Bettge and D.P. Abraham, *J. Electrochem. Soc.*, 159 (2012) A2109-A2117.
30. S.S. Zhang, *Electrochem. Commun.*, 8 (2006) 1423-1428.
31. M.H. Fu, K.L. Huang, S.Q. Liu, J.S. Liu and Y.K. Li, *J. Power Sources*, 195 (2010) 862-866.
32. Z. Chen, J. Liu and K. Amine, *Electrochem. Solid St.*, 10 (2007) A45-A47.
33. B. Yang, C. Li, J. Zhou, J. Liu and Q. Zhang, *Electrochim. Acta*, 148 (2014) 39-40.
34. S. Wilken, S. Xiong, J. Scheers, P. Jacobsson and P. Johansson, *J. Power Sources*, 275 (2015) 935-942.
35. R-S. Kühnel, N. Böckenfeld, S. Passerini, M. Winter and A. Balducci, *Electrochim. Acta*, 56 (2011) 4092-4099.
36. L. Zhang, Y. Ma, X. Cheng, P. Zuo, Y. Cui, T. Guan, C. Du, Y. Gao and G. Yin, *Solid State Ionics*, 263 (2014) 146-151.
37. J.Q. Zhang, *Electrochemical Measurement Technology*, Chemical Industry Press, Beijing (2010).
38. J.M. Zheng, Z.R. Zhang, X.B. Wu, Z.X. Dong, Z. Zhu and Y. Yang, *J. Electrochem Soc.*, 155 (2008) A775-A782.
39. C.L. Tan, H.J. Zhou, W.S. Li, X.H. Hou, D.S. Lü, M.Q. Xu and Q.M. Huang, *J. Power Sources*, 184 (2008) 408-413.
40. C. Yu, G. Li, X. Guan, J. Zheng, D. Luo and L. Li, *Phys. Chem. Chem. Phys.*, 14 (2012) 12368-12377.
41. N-S. Choi, K.H. Yew, H. Kim, S.S. Kim and W.U. Choi, *J. Power Sources*, 172 (2007) 404-409.
42. L. Zhao, J. Yamaki and M. Egashira, *J. Power Sources*, 174 (2007) 352-358.